THE EFFECT OF HARDENING OBTAINED AFTER TIG REMELTING ON THE RESISTANCE OF THE 7075 ALLOY STRUCTURE TO CAVITATION EROSION

Ilare BORDEASU [1], Brandusa GHIBAN [2, *], Cristian GHERA [3], Cornelia Laura SALCIANU [4], Lavinia Madalina MICU [5], Daniel Catalin STROITA [6, *,] Mihai Alin DEMIAN [7, *], Andreea Daniela BUZATU [8]

The phenomenon of cavitation is present in all areas of industry where liquids are in motion. The recognition of its effects is given by the destruction of the material structure through erosion, by vibrations and noise, as well as by the modification of the hydrodynamic field leading to a decrease in energy performance (efficiency). Correlated with the current trends in the use of aluminum alloys in various components, such as boat engine propellers and cooling pump rotors of car mills, the problem arises of improving the characteristics that determine their increased resistance to cavitation erosive stresses. In this regard, the paper presents the results of research into the behavior and resistance to erosion by vibratory cavitation of the structure of the 7075 aluminium alloy in the T651 state hardened by TIG remelting. Comparing the results obtained with those obtained on the semi-finished structure and obtained through artificial aging heat treatment regimes, shows a significant increase in the resistance of the structure to the cyclic stresses of the microjets developed by the hydrodynamics of vibrating cavitation.

Keywords: aluminum alloy type 7075, cavitation erosion, erosion depth, average erosion rate, microstructure.

* Corresponding author

[1] Professor, Dept. of Mechanical Machines Equipment and Transportation, University POLITEHNICA of Timisoara, Romania, ilarica59@gmail.com

[2] Professor, Dept. of Metallic Materials Science and Physical Metallurgy Department, University POLITEHNICA of Bucharest, Romania, brandusa.ghiban@upb.ro

[3] Lector, Dept. of Mechanical Machines Equipment and Transportation, University POLITEHNICA of Timisoara, Romania, cristian.chera@upt.ro

[4] Lector, Dept. of Mechanical Machines Equipment and Transportation, University POLITEHNICA of Timisoara, Romania, laura.salcianu@@upt.ro

[5] Assoc. professor, Department of Agricultural Technologies-Department I, King Mihai I University of Life Sciences, Timisoara, Romania, lavimicu@yahoo.com

[6] Conferentiar, Dept. of Mechanical Machines Equipment and Transportation, University POLITEHNICA of Timisoara, Romania, daniel.stroita@upt.ro

[7] PhD student, Dept. of Metallic Materials Science and Physical Metallurgy, University POLITEHNICA of Bucharest, Romania, demianalin96@gmail.com

[8] PhD student, Dept. of Metallic Materials Science and Physical Metallurgy, University POLITEHNICA of Bucharest, Romania, buzatuandreead@gmail.com

1. Introduction

The rapid pace of development of industrial equipment, with high requirements for technological mechanical processing capacity, mechanical characteristics, resistance to corrosive actions of the working environment and low specific mass, has led scientists to turn their attention to aluminum alloys, such as duralumin, rolled or cast, which largely meet these requirements [1-11].

Currently, there is practically no field in which a part or the subassembly made of aluminum or duralumin cannot be found. Among the most well-known applications, in which these alloys are present in at least one part, are [1, 2, 4, 11-14]: strength structures in the military, aeronautical, automotive, river and maritime fields, sports equipment, hydro-pneumatic and medical equipment.

The increase in mechanical, hydrodynamic and corrosive stress conditions has required the development of technologies, such as volumetric and surface heat treatments, to give duralumin the necessary properties. If, in the past, duralumin was used to manufacture parts subject to low or no mechanical stress (static or dynamic), we currently find it in highly stressed resistance structures, such as equipment that works in cavitation conditions with various intensity regimes [1-10]. As the range of duralumin alloys, in semi-finished states, is wide, the recent researches [1, 2, 4, 15-22] are oriented towards the development of technologies that give the surface structures of parts the necessary resistance to the erosion produced by the cavitation regime, such as that of thermal engines (valves, pistons, cooling pump rotors), household pumps and boat engine propellers. Among these alloys, the behavior and structural strength of the 7075 alloy in the T451 state to the stresses of cavitational microjets is very little known, although it is used in strength structures, in the military and aeronautical fields, where mechanical properties, especially hardness, close to those of low-alloy carbon steels are required [2, 11, 13, 14, 23-25]. In the literature, the only data on the cavitation resistance of the alloy 7075, cast or rolled, are those obtained at the Politehnica University of Timișoara, in the Cavitation Erosion Research Laboratory, which refer to the semi-finished states and those resulting from artificial aging heat treatments at 180ºC, 140ºC and 120ºC, [1, 2, 4, 26]. However, the analysis of these data does not provide a clear picture of the dependence of resistance and the behavior to cavitation stresses on the parameters of the treatment regime (temperature) and the values of mechanical properties. As a result, the research carried out by us on samples taken from cast semi-finished products of alloy 7075 T451 state, shows that the use of the TIG remelting method leads to an increase in the hardness of the stressed surface, with the effect of improving its behavior and resistance to cyclic cavitation stresses.

2. Material and Experimental Procedures

The researched material is the 7075 aluminum alloy in T451 condition, and cast state hardened by remelting using the TIG method. The reason for analyzing this alloy is that its behavior and resistance to cavity erosion were investigated for the cast semi-finished product state and for three structural states resulting from artificial aging heat treatments at [1, 4]: 180ºC, 140ºC and 120ºC, with a holding time of 12 hours and the desired increase in strength was not achieved, compared to the cast semi-finished product state. Wishing to expand its application to parts such as valves, distributors, boat propellers, pump rotors, which are part of the construction of hydraulic machines and equipment, which work in various intensities of cavitation, research was carried out on the structure of this alloy hardened by the TIG remelting method.

Chemical composition performed on the cast semi-finished product, in shown in table 1, and mechanical properties are given in table 2.

Table 1-

Chemical composition of the experimental aluminum alloy

alloy	Chemical composition,%wt.								
	Si	Fe	Cu	Mn	Mg	Cr	Zn	Ti	Al
Experimental	0.37	0.45	1.6	0.27	2.15	0.19	5.8	0.19	balance
7075	Max 0.40	Max 0.50	1.2-2.0	Max 0.30	2.1-2.9	0.18-0.28	5.1-6.1	Max 0.20	balance

Table 2-

Mechanical characteristics of the experimental aluminum alloy

alloy	Mechanical properties				
	Fracture strength, MPa	Yielding strength, MPa	Fracture elongation, %	Hardness, HB	Toughness, KCU, J/cm^2
experimental	225	175	6	74.5	9.5
7075, T451	Min 220	Min 163	Max 11	-	-

The remelting of the surface of the samples, which is attacked by cavitation, was done on the TIG welding machine, shown in Fig. 1. Working conditions and parameters of the technological regime used given in table 3.

Table 3

Parameter for welding process

Welding parameters	Curent, Is (A)	Voltage, Ua, (V)	Arc length, mm	Welding speed, cm/min	
	70	1.7	2	12	
	Linear energy, J/cm	Remelting time, s	Electrode, mm	Gas argon flow, L/min	Balancing, %
	10.4	15	2.4	8	60/40

The procedure for remelting the surface of the cavitation sample, according to technological recommendations, was: the base material was preheated to 100°C and the temperature between passes was maintained between 120°C and 150°C. To ensure a constant welding speed, the TIG welding head was mounted on a welding machine, thus mechanizing the process. To remelt the surface, parallel passes were made with a step between them equal to 2/3 of the width of a pass, thus ensuring an overlap of approximately 1/3 of the width of the pass. This allowed obtaining a smooth melted surface, without welding defects, such as lack of melting or marginal notches.

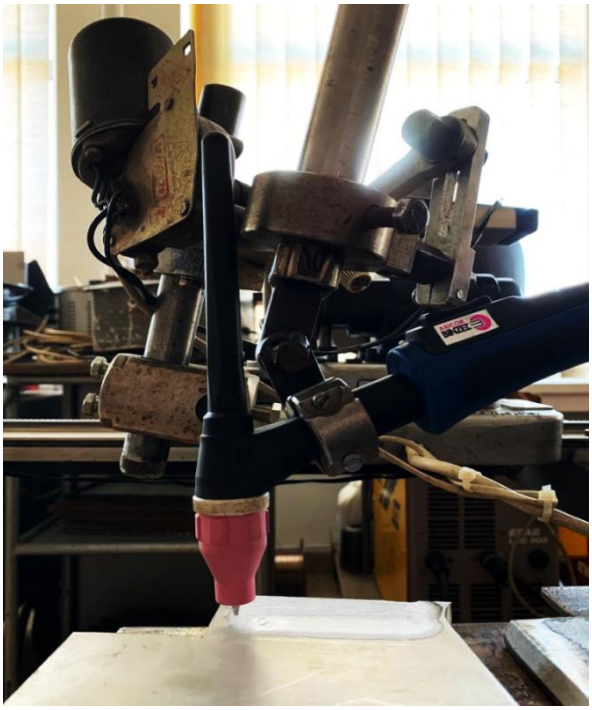

Fig. 1 Experimental stand used – TIG welding machine

The experimental research program was carried out on the vibrating apparatus with piezoceramic crystals [1, 2, 4, 9, 26, 27, 37] (see functional construction scheme of the apparatus in Fig. 2) using cylindrical samples with a diameter of 15.8 mm and a length of 16 mm. The experimental procedure and the research conditions were: the number of samples tested (three), the total duration of cavitation exposure (165 minutes), the intermediate periods (one of 5 and 10 minutes and 10 of 15 minutes each), the liquid medium (distilled water with a temperature of 22 ± 1ºC), the processing and interpretation of the recorded data, comply with the laboratory specifications [1-10, 27, 36] and the provisions of the international standard ASTM G32-2016 [38].

The mass losses, necessary for determining the average erosion depth during each intermediate cavitation period, were determined with the Kern ABT 100-5NM analytical balance, whose maximum weighing range is 100 g and the accuracy is 0.00001 g. The measurements were performed at an ambient temperature of 21...26°C and a humidity of 62...78 %.

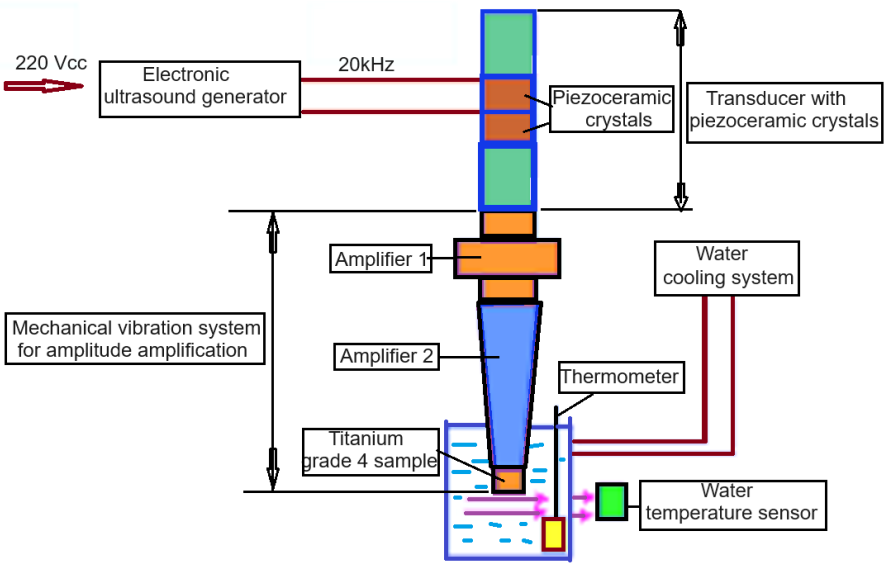

Fig. 2 Functional construction diagram of the vibratory device [adapted from [37]

3. Results and Discussions

3.1 Structural characterization of materials

Metallographic analysis of the structure, Fig. 3, performed with the REICHERT UnivaR microscope, shows that in the structure of this alloy the most common precipitates include $MgZn_2$ and Al_3Zn [1]. The macroscopic appearance of the samples, after TIG remelting is illustrated in Fig. 4. In Fig. 4b is presented the appearance after flat turning, grinding and finishing with abrasive paper to a roughness Ra = 3.2 μm.

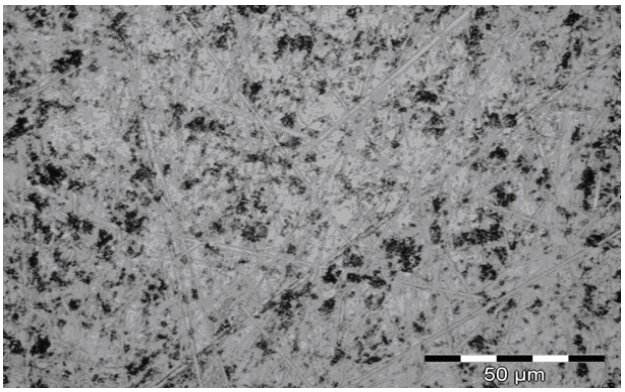

Fig. 3. Microstructural aspect of aluminum 7075 alloy in cast state

a) b)

Fig.4 Appearance of the sample surfaces after TIG remelting, a) image of the sample with the surface remelted by the TIG method, before cavitation testing
b) appearance of the remelted surface, prepared for hardness measurements and cavitation testing.

3.2 Mechanical behaviour

Hardness measurements, performed at 5 points on the surface of the sample for the experiment, led to an average value of 154 HB.

Since surface hardness is the property with the greatest influence on the resistance of the structure to cyclic fatigue stresses due to cavitational microjets [9, 26-36], after remelting and mechanical turning with grinding/polishing of the obtained flat surface, using the 251 VRSA AFFRI hardness tester. In strict accordance with the provisions of ASTM E384, the measurements of the hardness of the remelted layer were carried out in 5 points on the surface of the sample used for the experiment, resulting in an algebraic average value of 154 HB.

3.3. Cavitation Behaviour of Materials

According to ASTM G32-2016 standards, before the start of the cavitation test and after each intermediate period, the surfaces affected by cavitation were photographed with the HUAWEI 9 Nova phone and examined with the OPTICA

stereomicroscope, which allowed the visualization of the area affected by cavitation, as the evolution of the formed caverns and as an extension in the surface plane, due to the fact that the microscope allowed magnifications of 4x, 10x, 20x, 40x and 80x.

To assess the behavior of the TIG remelted surface structure during cavitation attack, the average cumulative erosion depths (MDEi) and the related average erosion penetration velocities (MDERi), were determined, using the mass losses of each intermediate period. With the determined values, with the relationships established in previous references [27, 39, 40] the specific cavitation curves MDE(t) and MDER(t) were constructed, which express the variations of the average cumulative erosion depths, Fig.5, and of the average erosion penetration velocity, Fig. 6, with the duration of exposure to cavitation. These curves, according to the laboratory's custom, were the basis for determining the parameters MDE_{max} and $MDER_s$, necessary for estimating the resistance of the surface structure to the cyclic stresses of cavitation microjets.

3.3.1 Specific diagrams of the structure's behavior during cavitation attack

The diagrams in Fig. 5 and 6 show both the analytical forms of the relationships with which the averaging curves of the experimental values were constructed, the values of the MDE_{max} and $MDER_s$, necessary parameters for evaluating the structure's resistance to cavitation erosion and the values of the statistical parameters that provide information about the accuracy of the experimental test and about compliance with the parameters of the TIG remelting technological regime - the average standard deviation σ and the degree of precision expressed by the tolerance interval, in which the averaged experimental values are distributed.

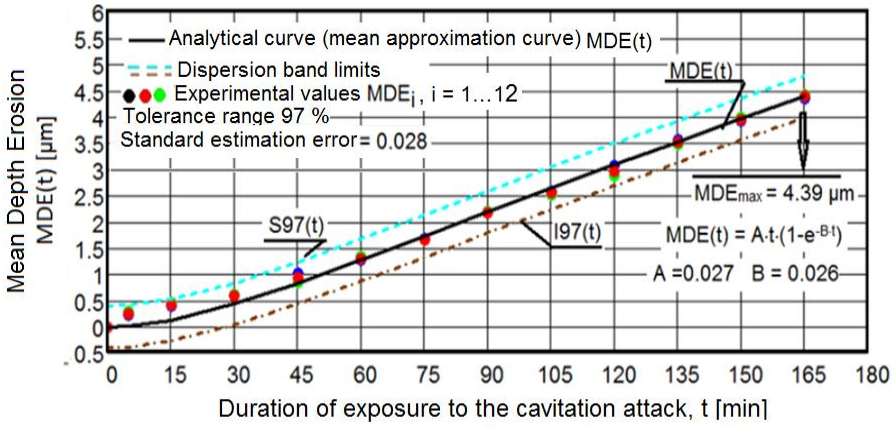

Fig. 5 Variation of the average cumulative erosion depth with the duration of cavitation exposure (***i*** = is the number of the intermediate period; the first of 5 minutes, the second of 10 minutes and the next ten of 15 minutes each)

The data in Fig. 5 shows:

- the three samples have similar behaviors, in some situations the cumulative material losses of the three samples, expressed by the cumulative average depths being equal (30 min, 75 min, 90 min, 135 min). These aspects show that for all three samples, the parameters of the TIG remelting technological regime were respected;
- an increase in MDE values is observed in the interval of 0...15 minutes, which suggests that from these moments the surface structure is eroded by cavitation. This suggestion is false, because, according to previous studies from the Cavitation Erosion Research Laboratory [27] and those provided by bibliographic references [31], this period (0...15) min is characterized by the elimination of the asperity peak, elasto-plastic deformations and the creation of crack networks;
- the limits of the 97% tolerance interval with the value of the average standard deviation $\sigma = 0.028$ show the accuracy of the experimental program, as a result of the rigorous control of the functional parameters of the vibratory device, through the software implemented in the computer with which the cavitation process was conducted;
- the averaging curve suggests an exponential increase with a linearization trend starting from minute 45. This evolution mode suggests two aspects: (1) damping of the impact pressures exerted by the cavitational microjets on the attacked surface, (2) increasing the hardness of the layer in the eroded structure.

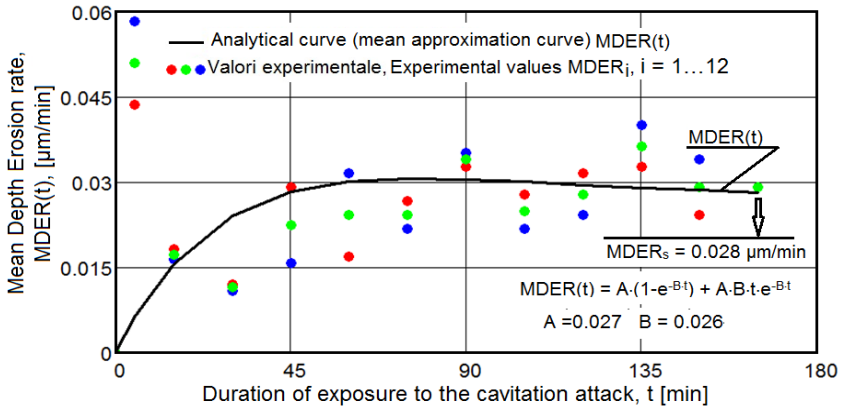

Fig. 6 Variation of the average erosion rate with the duration of exposure to the cavitation attack (***i*** = is the number of the intermediate period (the first of 5 minutes, the second of 10 minutes and the next ten of 15 minutes each)

From the data in Fig. 6 it can be seen:

- relatively small differences between the velocity values determined in the intermediate intervals, which confirm the hardness of the layer attacked by cavitation, obtained by TIG remelting;
- high values of the speeds in the first minutes (5 minutes), which confirm that the structure did not suffer significant losses of base metal, but that these values

are the effect of the elimination of abrasive dust and the tip of the asperities remaining after grinding;

- the relatively uniform dispersion of the experimental values compared to the averaging curve MDER(t), which reconfirms the accuracy of the experimental program, while simultaneously respecting the remelting regime of the layer required by cavitation.

3.3.2 Morphology of structural degradation

The morphology of the structural degradation is illustrated by photos and microfractographic images. The illustration of how the erosion caused by vibratory cavitation extends, both on the exposed surface and in depth, is shown in Fig. 7 by macro images of the surface appearance at 6 significant times, defined by the shapes of the curves MDE(t), Fig. 5 and MDER(t), Fig. 6. Comparing these images with the one from the minute zero - before the start of the test, Fig. 3b - the force, respectively the destructive intensity of the vibratory cavitation generated by the piezoceramic crystal device is noted.

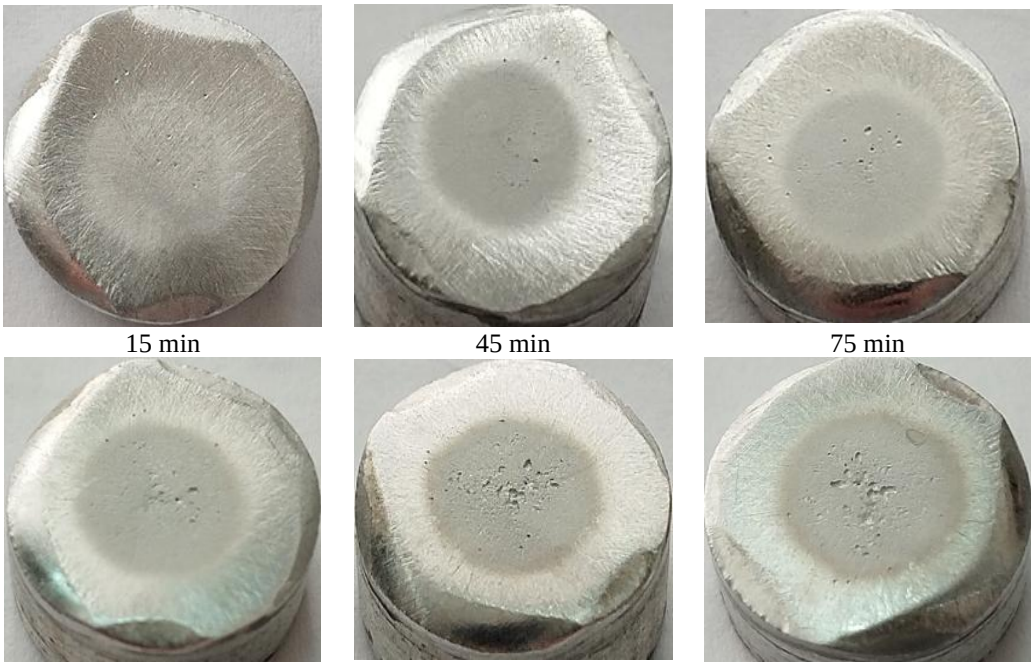

Fig. 7 Photographic images of the evolution of erosion in the sample surface structure (HUAWEI 9 Nova mobile phone)

The photographic images in Fig. 7 suggest that:

- the cavitation matting and incubation period is shorter, maximum 15 minutes.

The statement is supported by the image from 15 minutes, where microcaverns are already visible in the cavitated surface;

- increasing the duration of the cavitation attack leads to the development of caverns, of which the size and number increases;

- the shape of the caverns is pinched, with a crow-like appearance, which shows that the material was torn out and expelled under the shapes of the grains;

- starting with minute 105, the differences become increasingly difficult to notice, which explains the decrease in impact force, through the damping effect of the water and air that penetrated them, during the contraction period of the sonotrode.

To understand the mechanism of destruction of the surface structure, remelted by TIG, through the development of cracks with their transformation into microcavities, by cyclic cavitation stresses, fractography performed by scanning electron microscope (SEM), combined with energy dispersive X-ray spectroscopy (EDX), was used.

Figs. 8a and 8c show the obtained SEM images. They show that the alloy suffers from structural degradation through complex mechanisms that include mechanical fatigue, intergranular corrosion and localized plastic deformation.

The SEM images in Fig. 8a and Fig. 8b show the irregular shapes of the caverns, randomly distributed in the area affected by cavitation, and the image in Fig. 8c, a detail of the previous figures, shows a rough, spongy sponge-like surface. From the measurements made with the microscope, these caverns have small dimensions, from 10 μm to 50 μm. The shape of the caverns and the dispersion in the microscope objective, according to [1, 2, 4, 27, 31], classify the structure hardened by TIG remelting as one with a very high resistance to cavitation erosion.

The images in Fig. 8a also show that the deformations and caverns in the cavitated area appear to be localized in the central area where the cavities are present, indicating plastic deformation before fracture. The images in Fig.8b also show that the surfaces are relatively smooth around the edges, with a central area showing multiple cavities – material pull-outs. The sizes of the cavities vary and are evenly distributed in the central area. The edges of the samples show fine lines, suggesting possible cracks or deformation zones.

From the point of view of the degradation mechanism, we believe that the fracture has a mixed character, either ductile or brittle; ductile fracture being characterized by the formation of microvoids and plastic deformation before fracture, and brittle fracture occurring suddenly, with very little prior to the plastic deformation. The texture of the fractures is a general one, in which the microvoids are coalesced to form multiple cavities. SEM images show the presence of fine lines indicating intergranular (along grain boundaries) and transgranular (through grains) cracks. We believe that intergranularity indicates that grain boundaries were points of weakness, caused by the presence of impurities or secondary phases at these

boundaries. We also believe that transgranularity suggests a higher intrinsic strength of the grain boundary and may indicate a more homogeneous material. Based on microscopic analysis, we consider that the cavitation resistance of the analyzed structure is strongly dependent on the presence of impurities, phase segregation and local structural variability that can increase the susceptibility to cracking and breakage. In fig 9 is presented the EDS image with the dispersion of the chemical elements in the remelted and cavitated structure. The metallographic image in Fig. 10 shows the depths of the caverns in different areas, which exceed by over 40 times the calculated average MDEmax value (see Fig. 5), which supports the breaking force of the pressures developed upon impact of the structure with the cavitational microjets.

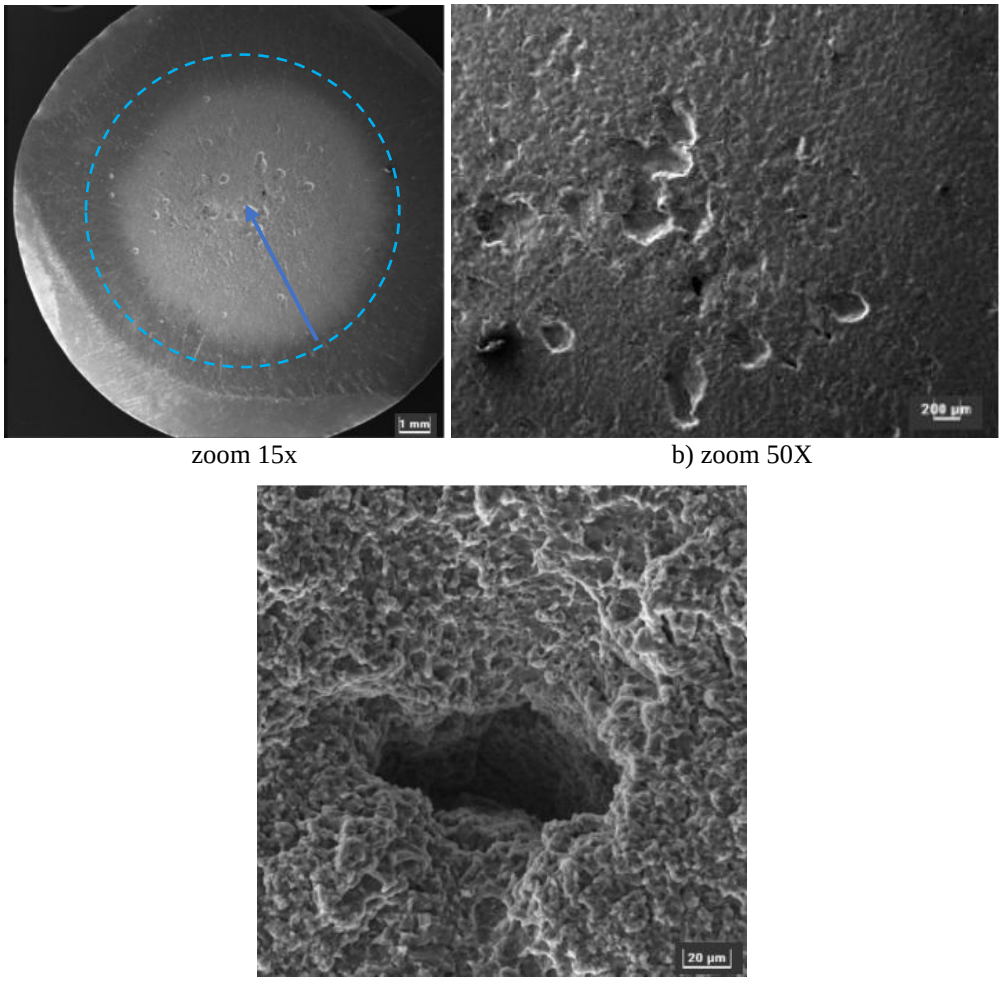

zoom 15x b) zoom 50X

c) zoom 1000X

Fig. 8 SEM analysis of the experimental specimens of alloy 7075, tested at cavitation after 165 hours at different microscope magnification powers

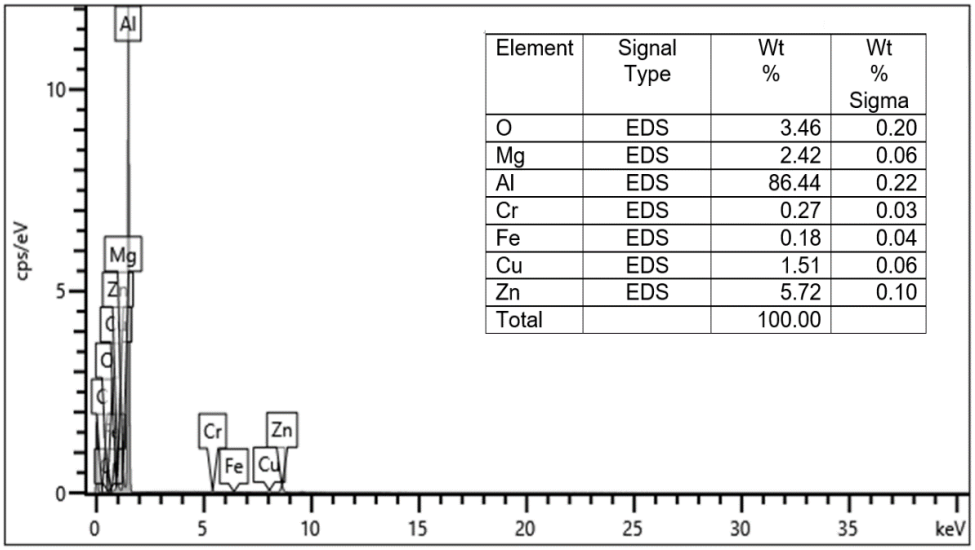

Element	Signal Type	Wt %	Wt % Sigma
O	EDS	3.46	0.20
Mg	EDS	2.42	0.06
Al	EDS	86.44	0.22
Cr	EDS	0.27	0.03
Fe	EDS	0.18	0.04
Cu	EDS	1.51	0.06
Zn	EDS	5.72	0.10
Total		100.00	

Fig. 9 EDS Imagine

3.3.3. Structural resistance to cavitation stresses

The assessment of the resistance of the remelted TIG structure to vibratory cavitation attacks, according to the data shown in the histogram in Fig. 11, is given by the values of the parameters MDE_{max} and $R_{cav} = 1/MDER_s$ (resistance of the structure to cavitation), compared with those of the structures of the same alloy for the semi-finished product state in the cast state and results from the volumetric heat treatments of artificial aging at 180ºC (TT180/12h), 140ºC (TT140/12h) and 120ºC (TT120/12h), with holding times of 12 hours.

The differences between these strengths are dictated by the differences in hardness values (74.55 HB for the cast semi-finished state [1], 91.3 HB for TT180/12h [4], 95.5 HB for TT140/12h [1] and 76.5 HB for TT120/12h [1]).

The histogram data shows an increase in the resistance to erosion caused by the cavitation phenomenon, conferred by TIG remelting, according to the values of the MDE_{max} parameter, from 63% compared to the structure obtained by the TT 180°C/12h artificial aging heat treatment to over 7 times compared to the structure obtained by the TT 120°C/12h. Also the values of the cavitation resistance parameter R_{cav}, show a significant increase, from 55% compared to the structure obtained by the TT 180°C/12h treatment, to over 8 times compared to the structure obtained by the 120°C/12h treatment.

Therefore, the application of TIG remelting technology to strengthen the hardness of the surface structure of the 7075 aluminum alloy is beneficial because it will lead to a substantial increase in its service life in hydrodynamic operating

environments, characterized by a strong cavitation regime, specific to pump rotors and motorboat propellers.

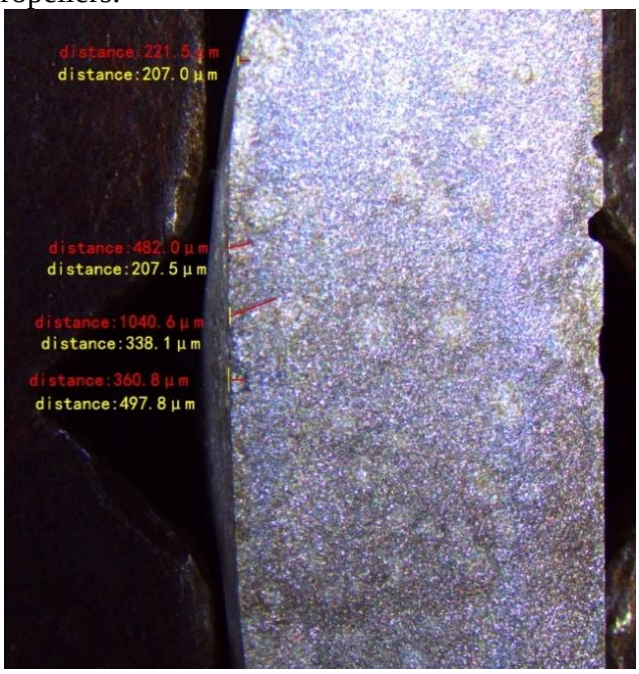

Fig.10 Structural appearance of maximum erosion penetration depth

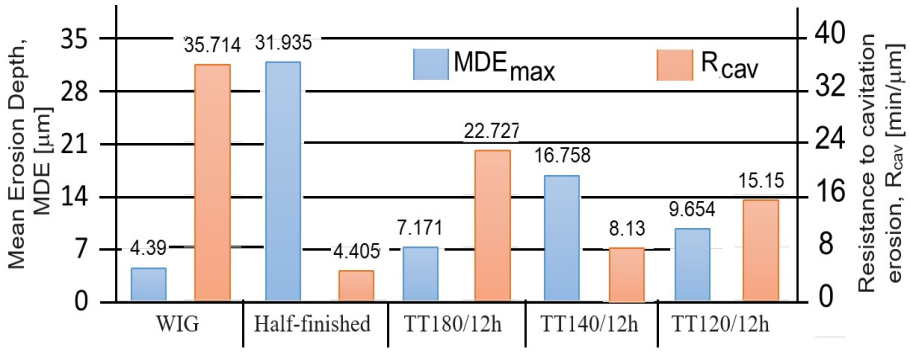

Fig. 11 Histogram of comparison of resistance to vibratory cavitation erosion

4. Conclusions

The evolutions of the specific MDE(t) and MDER(t) curves suggest that the structure obtained by TIG remelting of the surface stressed by cavitation, has a cavitation behavior specific to those with very good resistance to stresses.

From the point of view of resistance to cavitation erosion, due to the increase in hardness, the structure obtained by TIG remelting is clearly superior to the

structures of cast semi-finished products and to those obtained by heat treatments of artificial aging at 180ºC, 140ºC and 120ºC with holding times of one hour.

The microscopic analysis of the cavitation-eroded structure shows that the fracture is specific to fatigue stress, either ductile or brittle, characterized by the formation of microvoids and plastic deformation before fracture, followed by brittle fracture. It is caused by intergranular and transgranular crack networks formed under the forces developed by the impact of the surface with shock waves and microjets, generated by the hydrodynamic mechanism of cavitation. The shape of the crack networks and the location of their occurrence are influenced by brittle intermetallic compounds and the degree of impurity.

The research results show that the use of the TIG remelting method can be applied for the use of cast aluminum alloy 7075 in parts that work in cavitational currents with above-average destruction intensity, such as propellers for boat engines and pump rotors in the cooling system of thermal engines.

Acknowledgements

The experiments made in this paper are carried out both in University Politehnica Timisoara, Laboratories of Materials Science and Cavitation Erosion Research and National University of Science and Technology Politehnica Bucharest, Department of Metallic Materials Science and Physical Metallurgy.

R E F E R E N C E S

[1] *P.O. Odagiu*, Studii și cercetări experimentale privind comportarea mecanică și comportarea la eroziunea cavitațională a unui aliaj de aluminiu din seria 7075, Teza doctorat, UP Bucuresti, Romania, 2023.

[2] *D. Istrate*, Influența tratamentelor termice asupra comportarii unui aliaj din sistemul Al-Mg pentru aplicatii maritime, Teza doctorat, U.P Bucuresti, Romania, 2023.

[3] D. *Istrate, B.G. Sbârcea, Demian; A.M., A.D. Buzatu, L. Salcianu; I. Bordeasu, L.M. Micu, C. Ghera, B. Florea, B. Ghiban,* Correlation between Mechanical Properties—Structural Characteristics and Cavitation Resistance of Cast Aluminum Alloy Type Al-Mg. Crystals Vol. **12(11)**, 1538, 2022, DOI 10.3390/ cryst12111538.

[4] *A.N. Luca,* Cercetarea rezistenței la eroziunea prin cavitație a unor aliaje cu bază de aluminiu cu tratament termic de îmbătrânire artificială, Teza de doctorat, U.P. Timisoara, Romania, 2024.

[5] *I. Bordeasu, C. Ghera, D. Istrate, L. Sălcianu, B. Ghiban, D.V. Băzăvan, M.L. Micu, D.C. Stroita, A. Suta, I. Tomoiagă, A.N. Luca*, Resistance and Behavior to Cavitation Erosion of Semi-Finished Aluminum Alloy 5083, Hidraulica, no. **4**, pp.17-24, 2021.

[6] *I. Dionisie, C. Ghera, L. Sălcianu, I. Bordeașu, B. Ghiban, D.V. Băzăvan, L.M. Micu, D.C. Stroiță, D. Ostoia*, Heat Treatment Influence of Alloy 5083 on Cavitational Erosion Resistance, Hidraulica, no. **3**, pp.15-25, 2021.

[7] *A.N. Luca, I. Bordeasu, B. Ghiban, C. Ghera, D. Istrate, D.C. Stroiță*, Modification of the Cavitation Resistance by Hardening Heat Treatment at 450 °C Followed by Artificial Aging at 180 °C of the Aluminum Alloy 5083 Compared to the State of Cast Semi-Finished Product, Hidraulica, no. **1**, p.39-45, 2022.

[8] *D. Istrate, I. Bordeasu, B. Ghiban, B. Istrate, B.G. Sbarcea, C. Ghera, A.N. Luca, P.O. Odagiu, B. Florea, D. Gubencu*, Correlation between Mechanical Properties structural Characteristics and Cavitation Resistance of Rolled Aluminum Alloy Type 5083, Metals, Vol. **13**, Iss. 1067, 2023, DOI: 10.3390/met13061067.

[9] *A. N Luca, I. Bordeasu, B. Ghiban, A.M. Demian, C. Ghera,* Cavitation behavior study of the aging heat treated aluminum alloy 7075, Journal of Physics: Conference Series, (ICAS 2022), Vol. **2540**, Iss. 1, 2023, DOI 10.1088/1742-6596/2540/1/012037.

[10] *C. Ghera, O. P Odagiu, V. Nagy, L. M. Micu, A.N. Luca, I. Bordeasu, M. A. Demian, A. D. Buzatu, B. Ghiban*, Influence Of Ageing Time On Cavitation Resistance Of 6082 Aluminum Alloy, University Politehnica Of Bucharest Scientific Bulletin Series B-Chemistry And Materials Science, Vol. **84**, Iss. 4, 2022.

[11] *I. Mitelea*, Materiale inginereşti, Editura Politehnica, Timişoara, Romania, 2009.

[12] *A. Bej, I. Bordeasu, T. Milos, R. Badarau*, Considerations Concerning the Mechanical Strength of Wind Turbine Blades made of Fiberglass Reinforced Polyester, Materiale plastice, Vol. **49,** no.3, pp.212-218, 2012.

[13] *L.F. Mondolfo*, Aluminum Alloys: Structure and Properties, Ed. Elsevier, 2013.

[14] *J.R. Davis*, Aluminum and Aluminum Alloys, ASM International, 1993.

[15] *** Sun Cavity Advantage - Sun Hydraulics https://www.youtube.com/watch?v=yWNOO3r7sXo, Sun Cavity Advantage - Sun Hydraulics

[16] *** Aluminium alloys in shipbuilding – a fast growing trend https ://aluminiuminsider. com/aluminium-alloys-in-shipbuilding-a-fast-growing-trend/

[17] *D. C. Stroita, A. S. Manea, A. Cernescu*, Blade polymeric material study of a cross-flow water turbine runner, Materiale Plastice, Vol. **56**, Iss. 2, pp. 366 –369, 2019, DOI: 10.37358/MP.19.2.5187.

[18] *W. J. Tomlinson, S. J. Matthews*, Cavitation erosion of aluminium alloys, Journal of Materials Science, Vol**. 29**, pp. 1101-1108, 1994.

[19] *D. Bordeaşu, O. Proştean, I. Filip, F. Drăgan, C. Vaşar*, Mathematics, Vol.**10**, Iss 21, 2022.

[20] *D. Bordeasu, F. Dragan, I. Filip, I. Szeidert, G. O. Tirian*, Estimation of Centrifugal Pump Efficiency at Variable Frequency for Irrigation Systems, Sustainability, Vol. **16**, Iss 10, 2024.

[21] *D. Bordeasu*, Study on the implementation of an alternative solution to the current irrigation system, Acta Technica Napocensis-Series: Applied Mathematics, Mechanics, And Engineering, Vol. **65**, no.3s, 2022.

[22] *D.Tokar, C. Stroita, A. Tokar, A. Rusen*, Hybrid System that Integrat es the Lost Energy Recovery on the Water-Water Heat Pump Exhaust Circuit, IOP Conference Series: Materials Science and Engineering, Vol. **603**, no. 4, 042002, 2019.

[23] *C. Caplescu, L. Marsavina, I. Bordeasu, R. M. Sechei*, The Fracture of Polyurethane Materials in the Presence of Stress Concentrators, Materiale plastice, Vol. **47**, no.3, pp.379-382, 2010.

[24] *S. Vaidya, C. M. Preece*, Cavitation erosion of age-hardenable aluminum alloys, Vol. **9**, pp. 299–307, 1978.

[25] *N. I. Kolobnev, L. B. Khokhlatova D. K. Ryabov*, Structure, properties and application of alloys of the Al-Mg-Si-(Cu) system, Met. Sci. Heat. Treat., Vol. **53**, pp.440–444, 2012.

[26] *A. N. Luca, I. Bordeasu, L. M. Micu, B. Ghiban, C. Ghera, C. L. Salcianu, R. Badarau, D. Ostoia, M. Hluscu, N. A. Sirbu*, Evaluating the Cavitation Erosion of 7075-T651 Aluminum Alloy Heat Treated by Artificial Aging at 140 °C for 12 Hours, Solid State Phenomena,Vol. **S**, pp. 77 – 87, 2023.

[27] *I. Bordeasu*, Monografia Laboratorului de Cercetare a Eroziunii prin Cavitație al Universității Politehnica Timișoara (1960-2020), Editura Politehnica, ISBN 978-606-35-0371-9, Timisoara, 2020.

[28] *J. P. Frank, J. M. Michel,* Fundamentals of cavitation, Kluwer Academic Publishers-Dordrecht/Boston/London, 2004.
[29] *J. K. Steller,* International cavitation erosion test – test facilities and experimental results, 2 – emes Journees Cavitation, Paris, March, 1992.
[30] *J. M. Hobb,* Experience with a 20 – KC Cavitations erosion test, Erosion by Cavitations or Impingement, ASTM STP 408, Atlantic City, 1960.
[31] *J. P. Franc, J .L. Kueny, A. Karimi, D. H. Fruman, D. Fréchou, L Briançon-Marjollet. J. Y. Yves Billard, B. Belahadji, F. Avellan, J. M. Michel,* La cavitation. Mécanismes physiques et aspects industriels, Press Universitaires de Grenoble, Grenoble, France, 1995.
[32] *R. Garcia, F. G. Hammitt, R. E. Nystrom,* Corelation of cavitation damage with other material and fluid properties, Erosion by Cavitation or Impingement, ASTM, STP 408 Atlantic City, 1960.
[33] *J. M. Hobbs,* Vibratory cavitation erosion testing at nel, Confernce Machynery Groop, Edinburgh, 1974.
[34] *M. Bărglăzan, C. Velescu, T. Miloş, A. Manea, E. Dobândă, C. Stroiţă*, Hydrodynamic transmission operating with two-phase flow, WIT Transactions on Engineering Sciences, Open Access, 4th International Conference on Computational and Experimental Methods in Multiphase and Complex Flow, Bologna, 12 - 14 June, Vol. **56**, pp 369 – 378, 71370, 2007.
[35] *N. Tian, G. Wang, Y. Zhou, K. Liu, G. Zhao, L. Zuo*, Study of the Portevin-Le Chatelier (PLC) Characteristics of a 5083 Aluminum Alloy Sheet in Two Heat Treatment States, States Mater. Vol. **11**, 1533, 2018.
[36] *I. Bordeasu,* Cavitation erosion on materials used in the construction of hydraulic machines and naval propellers. Scale effects (in Romanian:Eroziunea cavitaţională asupra materialelor utilizate în construcţia maşinilor hidraulice şi elicelor navale. Efecte de scară), PhD Thesis, Timişoara, 1997.
[37] *O. Oanca,* Tehnici de optimizare a rezistenţei la eroziunea prin cavitaţie a unor aliaje CuAlNiFeMn destinate execuţiei elicelor navale, Teza de doctorat, Timișoara, Romania, 2014.
[38] *** ASTM, Standard G32; Standard Method of Vibratory Cavitation Erosion Test. ASTM: West Conshohocken, PE, USA, 2016.
[39] *I. Bordeaşu, M. O. Popoviciu, C. Patrascoiu, V. Bălăsoiu*, An Analytical Model for the Cavitation Erosion Characteristic Curves, Scientific Buletin Politehnica University of Timisoara, Transaction of Mechanics, Tom 49(63), Timişoara, pp. 253-258, 2004.
[40] *L.M. Micu, I. Bordeasu, M.O. Popoviciu*, A New Model for the Equation Describing the Cavitation Mean Depth Erosion Rate Curve", Rev. Chim. (Bucharest),Vol. **68**, no. 4, pp. 894-898, 2017
[41] *D. P. Mutascu*, Microstructura și rezistența la eroziune prin cavitație a unor straturi depuse prin sudare pe oțeluri inoxidabile Duplex, Teza de doctorat, Timișoara, Romania, 2024.